

## METHODS: ORIGINAL ARTICLE

# Proliferation of Genetically Modified Human Cells on Electrospun Nanofiber Scaffolds

Mandula Borjigin<sup>1</sup>, Bryan Strouse<sup>1</sup>, Rohina A Niamat<sup>1</sup>, Pawel Bialk<sup>1</sup>, Chris Eskridge<sup>1</sup>, Jingwei Xie<sup>2</sup> and Eric B Kmiec<sup>1</sup>

Gene editing is a process by which single base mutations can be corrected, in the context of the chromosome, using single-stranded oligodeoxynucleotides (ssODNs). The survival and proliferation of the corrected cells bearing modified genes, however, are impeded by a phenomenon known as reduced proliferation phenotype (RPP); this is a barrier to practical implementation. To overcome the RPP problem, we utilized nanofiber scaffolds as templates on which modified cells were allowed to recover, grow, and expand after gene editing. Here, we present evidence that some HCT116-19, bearing an integrated, mutated enhanced green fluorescent protein (eGFP) gene and corrected by gene editing, proliferate on polylysine or fibronectin-coated polycaprolactone (PCL) nanofiber scaffolds. In contrast, no cells from the same reaction protocol plated on both regular dish surfaces and polylysine (or fibronectin)-coated dish surfaces proliferate. Therefore, growing genetically modified (edited) cells on electrospun nanofiber scaffolds promotes the reversal of the RPP and increases the potential of gene editing as an *ex vivo* gene therapy application.

*Molecular Therapy–Nucleic Acids* (2012) 1, e59; doi:10.1038/mtna.2012.51; published online 4 December 2012

Subject Category: Method

## Introduction

Nanotechnology has already had a broad-based impact on medical research. Novel nanomaterials have been used to support and accelerate wound healing, repair damage caused by myocardial infarction, and improve bone and cartilage growth after injury.<sup>1,2</sup> This type of tissue engineering centers on the concept that natural or synthetic material can be used as a scaffold on which cells can proliferate in a conducive growth environment. Nanofibers are often used to construct these scaffolds which can be implanted in the body to enable restoration of normal human tissue integrity. Their functionality is due in large part to their high surface area and porosity which enhances cell adhesion capacity. The similarity of their 3D architecture to natural extracellular matrix also provides an excellent micro/nano environment within which cells can grow and function.<sup>3</sup>

Electrospun nanofibers have been shown to support growth and proliferation of a wide variety of cell types, including mouse fibroblasts,<sup>4,5</sup> human bone marrow-derived mesenchymal stem cells,<sup>6–11</sup> human satellite cells, rodent myoblast cells,<sup>12</sup> embryonic stem cells,<sup>13</sup> neural stem cells,<sup>14,15</sup> and neurite extension.<sup>16</sup> In particular, biodegradable scaffolds fabricated from synthetic polymers, such as polycaprolactone (PCL), are excellent choices for cell growth and tissue engineering due to the ease of electrospinning and biocompatibility.<sup>17–21</sup> PCL nanofiber scaffolds facilitate mouse embryonic stem cells to differentiate into specific neural lineages, specifically neurons, oligodendrocytes, and astrocytes, and promote and guide the neurite outgrowth.<sup>13,16</sup> While the electrospun

nanofiber scaffolds are prevalent in cell culture and tissue engineering, their application to the growth of genetically modified cells has not yet been examined.

Over the course of the last 10 years, it has become increasingly apparent that a single nucleotide in the human genome can be specifically and uniquely changed by a technique widely known as gene editing (see ref. 22 and references therein). This type of nucleotide exchange can be catalyzed by oligonucleotide-directed gene modification,<sup>23–30</sup> zinc finger nuclease genomic modification,<sup>31,32</sup> and transcription activator-like effector nuclease-directed DNA targeting<sup>33,34</sup> among others. The differences among these techniques lie in the mechanism by which the exchange is executed. Zinc finger nucleases and transcription activator-like effector nucleases use sequence and structural recognition motives to locate the target and induce a break in the chromosome. This event is followed by DNA repair and recombination activity which act to repair the scission.<sup>35</sup> In contrast, oligodeoxynucleotides (ODNs) direct gene editing by initially aligning in homologous register with a complimentary region in the gene, most often in areas of active DNA replication.<sup>36,37</sup> These ODNs are purposely designed so that, once hybridized at the target site, a single mismatched base pair is created between the mutant target base in the cell's genome and the ODN itself. Subsequently, the mismatched base will be corrected by mismatch repair enzymes or through direct integration into an actively replicating region of the chromosome.<sup>37</sup>

By its very nature, the process of ODN-directed gene editing requires a large number of free DNA ends that are delivered into the cell and activate the DNA damage response

<sup>1</sup>Department of Chemistry, Delaware State University, Dover, Delaware, USA; <sup>2</sup>Marshall Institute for Interdisciplinary Research, Marshall University, Huntington, West Virginia, USA. Correspondence: Eric B Kmiec, Professor and Chairman, Delaware State University, Department of Chemistry, 1200 N. DuPont Highway, Science Center South Room 312, Dover, Delaware 19901, USA. E-mail: [ekmiec@desu.edu](mailto:ekmiec@desu.edu)

**Keywords:** electrospun; gene editing; nanofiber; ssODN

Received 5 July 2012; accepted 1 October 2012; advance online publication 4 December 2012. doi:10.1038/mtna.2012.51

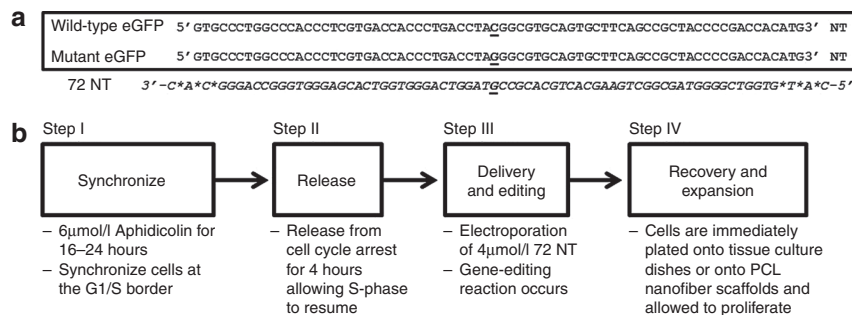


**Figure 1 HCT116-19 gene-editing model system.** (a) The mutant eGFP gene segment with the target codon located in the center of the sequence is displayed, and the nucleotide targeted for exchange is underlined. The sequence of 72 NT, which is used to target the nontranscribed (NT) strand of the eGFP mutant gene is shown below the mutant eGFP gene sequence. (b) The experimental design of the standard gene-editing reaction including the detailed steps, synchronization, release, delivery and editing, and recovery and expansion, are presented. eGFP, enhanced green fluorescent protein; PCL, polycaprolactone.

checkpoint proteins, CK1 and CK2, respectively.<sup>38</sup> DNA replication is slowed or halted by the normal action of this pathway because an abundance of free ends resembles broken genomic DNA. Eventually, the cell reduces the ODN level by clearance and these proteins are “deactivated”. But, as a result of the activation, the targeted cell appears to enter a quiescent state of growth.<sup>39</sup> Such stress responses along with the physical harm incurred by the process of electroporation itself result in a long recovery phase which we have termed the reduced proliferation phenotype (RPP).<sup>23,24,38–42</sup> Clearly, until the RPP is reversed, applications of gene editing, no matter what technique is used to direct the change, will be severely hindered. In this study, we used an HCT116-19 cell line as a model system to investigate how electrospun PCL nanofiber scaffolds might impact the survival and proliferation of genetically modified cells. Our data show that genetically modified HCT116-19 cells recover on polylysine-coated aligned PCL nanofiber scaffold and proliferate vigorously, enabling the reversal of RPP.

## Results

### RPP of gene-corrected HCT116-19 cell line

We used a modified HCT116 cell line (HCT116-19) as a model, a system in which the integrated single point mutated eGFP gene is corrected, resulting in the emergence of green fluorescent cells. A specific sequence 72-mer (single-stranded ODN (ssODN)) was designed to edit the single base mutation in the integrated eGFP gene, enabling the expression of the functional GFP after correction (Figure 1a). The basic experimental design, outlined in Figure 1b, is based on the electroporation of the 72 nontranscribed (NT) ODN into synchronized and released (for 4 hours) HCT116-19 cells bearing a single integrated copy of the mutant eGFP gene (eGFP<sup>-</sup>). To achieve a robust level of gene-editing efficiency, we used 4 μmol/l 72 NT ssODN and  $5 \times 10^5$  cells in these experiments.<sup>41</sup> Gene-editing efficiency was then monitored from 24 hours through 168 hours (8th day), conducting fluorescence-activated cell sorting (FACS) analysis on triplicate samples every day. As shown in Figure 2, the correction efficiency was about 2.46% after 24 hours, the highest level among the seven timepoints examined. The correction efficiency decreased to 2.11% at 72 hours, and to 0.42% at 144 hours. At 168-hour timepoint, the percentage of corrected cells dropped to 0.26%. Presumably, the correction efficiency,

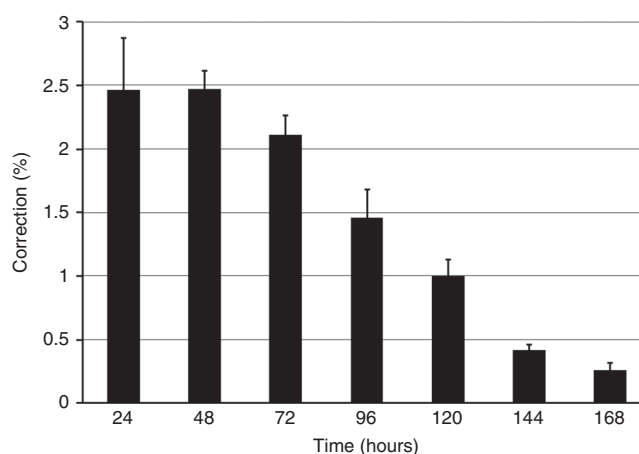


**Figure 2 Cell recovery and proliferation of genetically modified cells on plain surface of 6-well dishes over an extended time course.** HCT116-19 cells were synchronized with 6 μmol/l aphidicolin for 24 hours, released for 4 hours, and targeted with 4 μmol/l 72 NT ssODN. Twenty-one gene-editing reactions were carried out simultaneously, and cells of three samples were harvested every 24 hours over the 7-day time course. FACS analysis for gene-editing efficiency was performed using a Guava EasyCyte 5HT Flow Cytometer. Correction efficiency at each timepoint (hours) is exhibited. The statistical analysis was performed by analysis of variance. FACS, fluorescence-activated cell sorting; NT, nontranscribed; ssODN, single-stranded oligodeoxynucleotide.

or percentage of corrected cells in the sample, should stay the same if both gene-corrected and uncorrected cells maintain a similar proliferation rate. But, the corrected cells do not exhibit similar proliferation rates when compared with normal uncorrected cells. In fact, a steady decrease in the percentage of corrected cells within the population is observed over time. The gradual “dilution” of cells bearing the corrected eGFP<sup>-</sup> gene reflects the RPP discussed above. This reduction is not due to a disproportionate loss of viability but rather a preponderance of corrected cells that apparently remain in a quiescent-like state and do not divide.<sup>43</sup>

### PCL nanofiber scaffolds and their interaction with HCT116-19 cells

A variety of cell types adhere to non-woven electrospun nanofiber scaffolds, and the use of the nanofiber scaffolds are

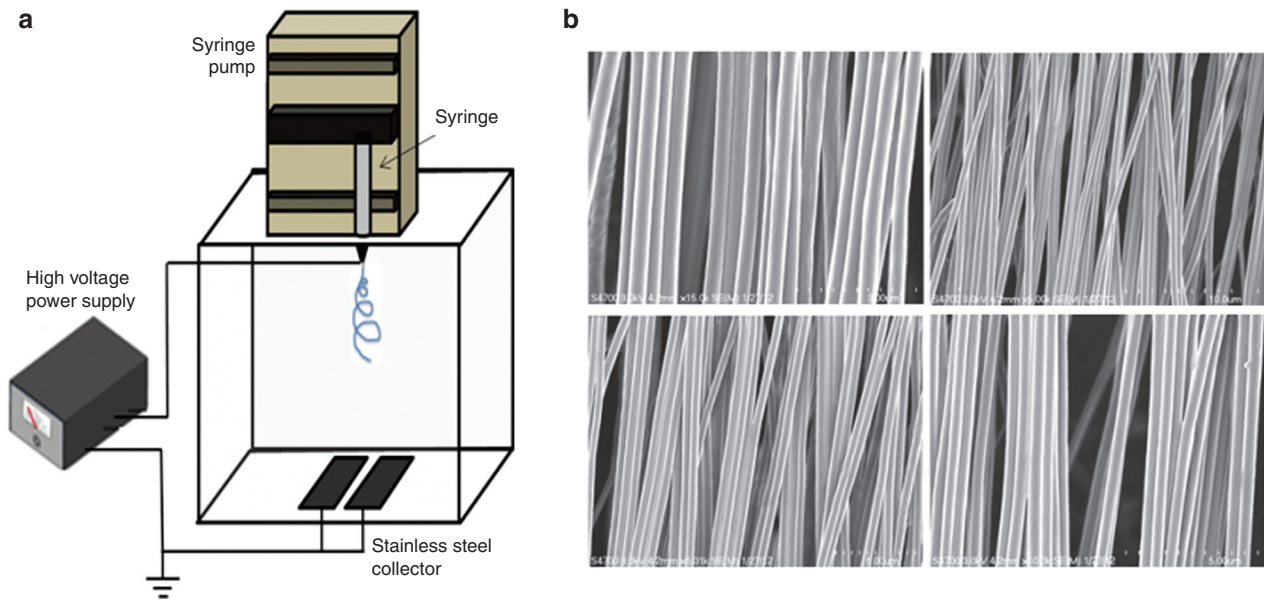


**Figure 3 Electrospraying instrumentation and SEM images of PCL nanofiber scaffolds.** (a) The instrumentation consists of a syringe with spinneret, a syringe pump, a high voltage power supply, and a nanofiber gap collector. (b) Scanning electron microscopy (SEM) images of parallel aligned PCL nanofiber scaffolds that were taken using a field-emission scanning electron microscope (S4700; Hitachi, Tokyo, Japan). Nanofibers were electrospun on the gap collector by adjusting flow rate of PCL solution at 0.5 ml/hour using a syringe pump while a potential of 12 kV was applied between the spinneret (a 22-gauge needle) and a grounded collector located 12 cm away. NT, nontranscribed; PCL, polycaprolactone.

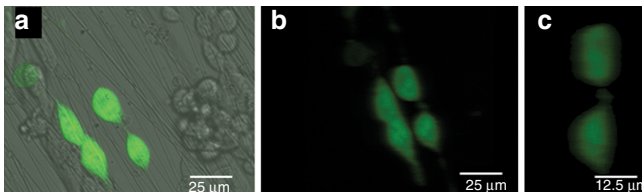


**Figure 4 Attachment of eGFP<sup>+</sup> HCT116-19 cells onto PCL nanofibers.** (a) HCT116-19 cells ( $1 \times 10^6$ ) that have undergone gene editing with 72 NT were plated onto a polylysine-coated electrospun PCL nanofiber loose membrane. Forty-eight hours after the plating, cells were observed under a Leica SP5 TCSII multiphoton confocal microscope. Cells expressing eGFP were found on nanofibers in a typical view. (b) Confocal image of the four (created) cells expressing eGFP (side view, b), showing the flatter side of cells attached to the nanofiber and the bulgy free surface of the cells. (c) Image of the same two cells on the right (side view) at a higher magnification ( $\times 40$  objective). eGFP, enhanced green fluorescent protein; NT, nontranscribed; PCL, polycaprolactone.

prevalent in tissue engineering. PCL nanofiber scaffolds exhibit excellent support for cell attachment and differentiation,<sup>16,19–21</sup> a feature that drew our attention to apply these templates to the RPP problem. We fabricated PCL nanofiber scaffolds with 10% PCL solution in a mixture of dichloromethane and N,N-dimethylformamide solvents using our standard electrospraying apparatus (Figure 3a). The electrospun PCL nanofibers were parallel aligned without defects and their average diameter was about 500 nm (Figure 3b). Since the PCL polymer is hydrophobic, we oxidized the surface of the nanofibers with oxygen plasma treatment, and coated them with 0.1% aqueous polylysine solution for the enhancement of cell adherence. We then performed a gene-editing reaction with  $1 \times 10^6$  HCT116-19 cells and 4  $\mu\text{mol/l}$  ssODN, using the standard

protocol, and plated the cells onto polylysine-coated PCL nanofiber scaffolds in 6-well dishes.

Twenty-four hours after culturing the HCT116-19 cells on PCL nanofiber scaffolds, we monitored gene editing and cell morphology. The fluorescence intensity of the eGFP-corrected HCT116-19 cells is normally bright after 48 hours (or the 3rd day) in our experience. Cells that were found on the nanofiber scaffolds adhered onto the nanofibers tightly and elongated along the nanofiber orientation, demonstrating an influence of the nanofiber topology on the morphology and spatial relationship of the cells (Figure 4a,b). HCT116-19 cells that grew along individual strings of sparsely distributed PCL nanofibers were transformed morphologically that they exhibit a healthy spindle shape. We took a series of confocal images of two corrected cells, and found that not only did the cells exhibit a spindle shape, but also they hung from a PCL nanofiber showing the saggy side opposite to the nanofiber (Figure 4c). Comparatively, HCT116-19 cells grown on polylysine-coated dish surfaces did not show elongation or transformation, maintaining their original morphology (Figure 5). Morphological transformation, due to an interaction between nanofibers and cells, implies that physiological stimuli<sup>16,20,44</sup> of the PCL nanofiber scaffolds may have enabled the growth of gene-edited HCT116-19 cells.

#### Cell proliferation on PCL nanofiber scaffolds

The cell morphological change triggered by the interaction between an individual PCL nanofiber string and HCT116-19 cells led us to ask whether the electrospun PCL nanofiber scaffolds can support the recovery and proliferation of gene-edited HCT116-19 cells. To address this question, we seeded the  $1 \times 10^6$  HCT116-19 cells which had undergone

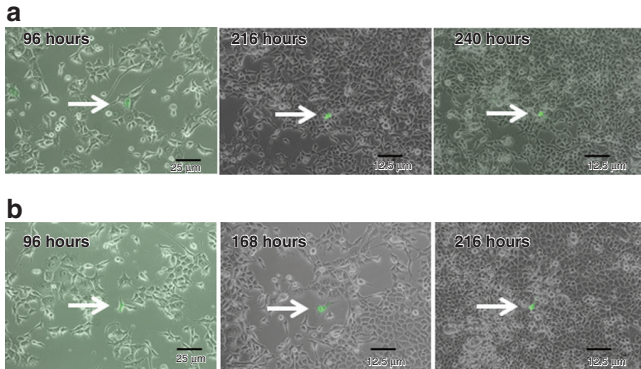


**Figure 5 Genetically modified HCT116-19 cells plated onto polylysine-coated 6-well dishes for recovery and proliferation.** (a) HCT116-19 cells ( $1 \times 10^6$ ) that have undergone gene editing with 72 NT were plated onto polylysine-coated 6-well dishes. Cells were monitored between 96 and 240 hours, and imaged using a Zeiss Axiovert 25 CFL inverted light microscope (Zeiss). (b) HCT116-19 cells, treated in the same fashion as (in a) above, from an independent group of experiments were monitored and imaged between 96 and 216 hours using the same imaging strategy as in a. NT, nontranscribed.

gene editing onto the polylysine-coated PCL nanofiber scaffolds as described previously, and observed their division under a Zeiss fluorescence microscope (Zeiss, Oberkochen, Germany) daily. It is an empirical task to look for cell proliferation on paralleled PCL nanofiber scaffolds since not only do the cells cling onto the nanofibers but also they migrate along the nanofiber strings.<sup>20,44,45</sup>

Clusters of proliferating HCT116-19 cells were formed routinely on nanofiber scaffolds (Figure 6a,b). We believe that both the nanofiber interaction with cells and the cell density provide a conducive environment for growth. As shown in Figure 6a, four HCT116-19 cells were observed at one position, 96 hours after the gene-editing reaction was initiated. The corrected cells were nestled in a cluster of uncorrected cells and proliferated continuously within the cluster with monitoring up to 288 hours (Figure 6a). As a clear view of robust growth, we present a dark field view of the dividing cells from timepoint 72 hours through 336 hours (Figure 6b). Each of the image panels reveals a progressive increase in the number of eGFP-positive cells as a function of time, supporting the notion that incubation of genetically modified cells on nanofibers supports cell growth. Since the PCL nanofibers were parallel aligned to form the scaffold and the cell density was in the medium range, the proliferating cells possessed the morphological features of regularly dividing cells instead of spindle shape cells on individual nanofiber strings. In contrast, an abnormal transformation was observed for the HCT116-19 cells plated on a polylysine-coated surfaces from 48 hours onward. The corrected HCT116-19 cells plated on that surface died eventually at 96 hours, without any evidence of proliferation (Figure 5). While this supports our overall conclusion that nanofibers enable growth, it also suggests that cell density alone did not contribute to proliferation of genetically modified HCT116-19 cells.

#### Replication fork activity is restored in genetically modified cells when grown on PCL nanofiber scaffolds

The incorporation of modified nucleotides (BrdU) into the growing chain of DNA can be used to determine DNA

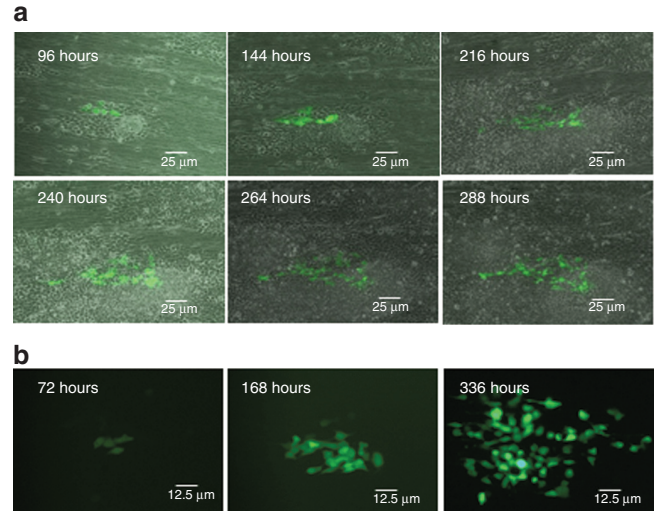


**Figure 6 Proliferation of genetically modified HCT116-19 cells on a polylysine-coated PCL nanofiber scaffold.** (a) HCT116-19 cells ( $1 \times 10^6$ ) that have undergone genetic modification with 72 NT were plated onto polylysine-coated electrospun PCL nanofiber scaffolds. Cells were monitored between 96 and 288 hours, and imaged using a Zeiss Axiovert 25 CFL inverted light microscope (Zeiss). The transmitted light and fluorescent images were overlaid to show both the nanofibers and the cells. (b) Genetically modified HCT116-19 cells plated on a polylysine-coated nanofiber scaffold from another group of experiment were monitored between 72 and 336 hours. In order to show the expansion of the genetically modified (eGFP<sup>+</sup>) cells in a clear view, only the dark-field view images were displayed in this sequence. eGFP, enhanced green fluorescent protein; NT, nontranscribed; PCL, polycaprolactone.

replication activity; in fact, it is one of the most sensitive, validated assays designed to do so. A variant of the BrdU assay, the Click-iT EdU kit, is an excellent tool to measure DNA replication fork activity. Incorporation of EdU in newly synthesized DNA can be detected by a fluorescent antibody, and the cells bearing EdU-incorporated DNA can be visualized by fluorescence microscopy. To further examine proliferation, we carried out an EdU uptake assay on cells plated onto either polylysine-coated PCL nanofiber scaffolds or onto polylysine-coated 6-well dish surfaces as described in Materials and Methods. Both eGFP<sup>+</sup> and eGFP<sup>-</sup> HCT116-19 cells proliferate robustly on nanofiber scaffolds as shown above in Figure 6a,b, respectively. We were able to observe the EdU incorporation readily in dividing corrected cells plated and recovered on the same nanofiber scaffolds used for assessing proliferation (Figure 7a). In contrast, the eGFP<sup>+</sup> cells recovered on polylysine-coated plain dish surfaces did not incorporate EdU into their DNA, while surrounding eGFP<sup>-</sup> (unedited) cells demonstrated active proliferation even in the culture plates (Figure 7b). These data clearly demonstrate that DNA replication, cell recovery, and proliferation are active within genetically modified cells grown on nanofiber scaffolds, but is not observed on cells plated on polylysine-coated plain dish surfaces. We wanted to compare the percentage of correction within a targeted cell population recovered on plain surface or PCL fibers. The same protocol that generated the data presented in Figure 2 was used and the cells recovered for 96 hours; after which time, the percentage of eGFP-positive cells was measured by FACS. As seen in Figure 8a, the

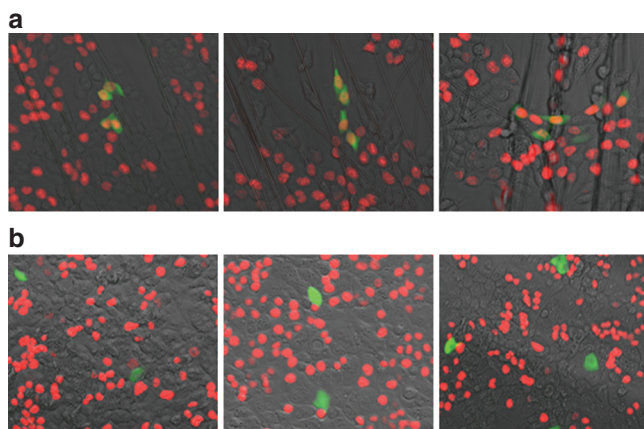


**Figure 7** DNA replication activity of eGFP<sup>+</sup> and eGFP<sup>-</sup> cells plated onto polylysine-coated nanofiber scaffolds or polylysine-coated PCL surfaces. (a) HCT116-19 cells ( $1 \times 10^6$ ) that were targeted with 72 NT for gene editing were plated onto a polylysine-coated PCL nanofiber scaffold for 72 hours. DNA replication activity was measured using the Click-iT EdU assay. The genetically modified cells (eGFP<sup>+</sup>) exhibit green fluorescence, and cells with active DNA replication display red due to incorporation of EdU into newly synthesized DNA. (b) HCT116-19 cells that have undergone genetic modification as described above were plated onto a polylysine-coated 6-well dish surface. The Click-iT EdU assay was carried out 72 hours after plating to measure the DNA replication activity, and the images were taken using EVOS FL microscope (AMG Micro). eGFP, enhanced green fluorescent protein; NT, nontranscribed; PCL, polycaprolactone.

level of correction observed with cells recovered on the plain surface is approximately the same as seen in the data from **Figure 2**. But, the percentage of cells exhibiting the eGFP-positive phenotype is significantly higher when the targeted cells are recovered for 96 hours on PCL nanofibers.

We extended this study one more step by removing cells from the fibers and placing them on a plain surface to observe the status of the corrected cells. After 48 hours of growth (total reaction time, 144 hours) on the plate, corrected cells were identified and photographed using the EVOS microscope (EVOS Microscopes, Bothell, WA). As seen in the three panels in **Figure 8b**, eGFP-positive cells extracted from the fibers, are viable and proliferate.

## Discussion

At the molecular level, gene editing is divided into two basic phases: initiation, in which the oligonucleotide aligns with its target site in the chromosome and, resolution, the phase in which the nucleotide exchange actually takes place.<sup>46</sup> The initiation of the reaction involves the creation of a D-loop wherein the ODN pairs with its complement and displaces its homolog. Genetic and biochemical evidence provide strong support for the existence and importance of this three-stranded complex.<sup>47</sup> But, the pathway to resolution in the second phase, which leads to the alteration in the DNA sequence, remains somewhat promiscuous and several scenarios are still possible.<sup>37</sup> The most widely well-accepted mechanism of the single-nucleotide exchange centers on the concept that DNA replication utilizes the aligned ODN within the D-loop, as a primer for extension of the growing strand.

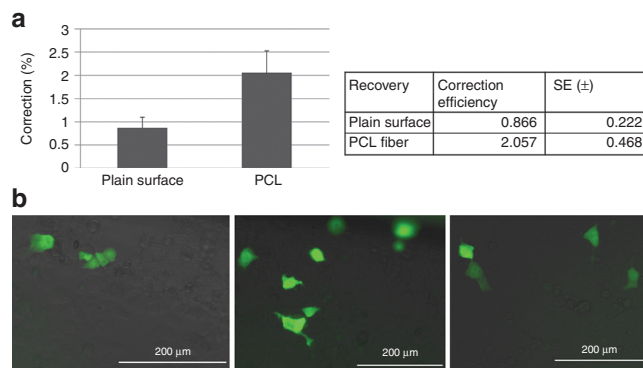


**Figure 8** Genetically modified HCT116-19 cells recovered on PCL can be expanded when replated on plain surfaces. (a) HCT116-19 cells were synchronized with 6  $\mu\text{mol/l}$  aphidicolin for 24 hours, released for 4 hours, and targeted with 6  $\mu\text{mol/l}$  72 NT ODN. FACS analysis for gene-editing efficiency was performed using a Guava EasyCyte 5HT Flow Cytometer after 96 hours. (b) HCT116-19 cells were synchronized with 6  $\mu\text{mol/l}$  aphidicolin for 24 hours, released for 4 hours, and targeted with 6  $\mu\text{mol/l}$  72 NT ssODN and plated on PCL and plain surface. After 96 hours, the cells were removed from PCL fiber using trypsin and plated on plain surface for another 48 hours. Cells were monitored after 48 hours and, imaged using EVOS FL microscope (AMG Micro). FACS, fluorescence-activated cell sorting; ssODN, single-stranded oligodeoxynucleotide; PCL, polycaprolactone.

Then, the replication fork passes through the site where the D-loop was formed, and the ODN effectively becomes part of the newly synthesized strand of DNA.<sup>25–29,37</sup> Thus, DNA replication plays an important role in the gene-editing reaction and the molecular events that contribute to the mechanism impact the efficiency and regulation of the exchange process quite dramatically.

At the cellular level, the gene-editing reaction can be broken down into three phases: Transfection, wherein the ODN is introduced in the cell; Recovery, in which the cells adjust to and recover from the presence of the ODN, restoring normal metabolic activity; and Expansion/Proliferation in which converted cells replicate their DNA and resume a normal proliferative rate. The characterization of phases I and III have been the focus of most current investigations which logically have been aimed at increasing gene-editing frequencies and isolating clones of modified cells.<sup>24</sup> Studies on phase I activities center around alterations in ODN design while those surrounding activity in phase III focus on trying to expand the rare clone of a modified cell.<sup>40</sup> It is generally accepted that cells that receive a lower dose of ODN can proliferate at a near-normal rate but do not contain the changed (new) base. Conversely, those cells containing a sufficient amount of ODN to enable gene editing, proliferate at a much reduced rate. This mass action effect can be tempered if the degree of chemical modifications on the ODNs is reduced or eliminated,<sup>26,28,36</sup> but the level of editing is again much lower; often three- to fivefold less than when the typical work horse phosphorothiotated ODN is used. This reduction in the number of modified cells will ultimately increase the difficulty of identifying and expanding the rare clonal isolates bearing an altered genome.

These observations have led us to speculate that the amount of ODN required to direct gene editing causes

adverse metabolic effects in the cells. One of these effects is the RPP in which genetically modified cells exhibit slow growth and can therefore be effectively “diluted out” by their unmodified counterparts. Yet, if we reduce the amount of ODN introduced into the cell, the level of correction falls precipitously.<sup>23,41,43</sup> This result would make it even more difficult to obtain a clonally isolated cell line. One solution is to remove the phosphorothioate modifications on the ODN to direct gene editing. This idea has significant merit and a less toxic effect on cell metabolism has been observed.<sup>36</sup> As such, the RPP may be partially averted. But, the overall level of correction is severely limited, and cells bearing the modified genotype are hard to locate, irrespective of their isolation and expansion.<sup>41</sup> As an alternative strategy, we have focused on the targeted cell itself in the hope that we could create conducive conditions that enable robust proliferation and reverse RPP induced by ssODNs. Based on previous studies centered around the effects that nanofibers have on cell growth,<sup>16,20,21,44,48</sup> we used PCL scaffolds as templates upon which to proliferate gene-edited cells.

Electrospun nanofibers, in particular, enable the proliferation of many types of cells. For example, PCL/collagen is a composite nanofiber often chosen for cell proliferation studies. Vascular tissue engineering showed that smooth muscle cell proliferation on the PCL/collagen nanofiber scaffold is significantly increased (up to 63, 73, and 82%) as compared with growth on PCL nanofiber scaffold alone.<sup>19,48</sup> Schwann cell migration, neurite orientation, and process formation have all been improved on PCL/collagen nanofibers and analyses of isolated sensory neurons revealed significantly better axonal guidance on PCL/collagen scaffolds.<sup>20</sup> We can now add the expansion of genetically modified HCT116 cells to the list of cell types known to be amenable to growth on nanofiber scaffolds. We believe that the recovery/expansion phases of the gene-editing reaction takes place because the nanofibers provide a conducive 3D growth environment with amenable topography. These structural conditions may resemble the arrangement cells encounter *in vivo* and thus proliferation is encouraged. It was obvious that eGFP<sup>+</sup> HCT116-19 cells grown on polylysine-coated nanofiber scaffolds exhibited robust proliferation compared with eGFP<sup>+</sup> cells grown on polylysine-coated dish surfaces (Figures 6,7,8). But, it is important to note that a percentage, not all, of the genetically modified cells actually expand during the time frame we have used in these experiments. In addition, PCL fibers are among the most commonly used type of nanofibers, but they may not be the most conducive for expansion of genetically modified cells; we are testing PCL composite fibers now in order to obtain fully robust recovery. Importantly, though, PCL nanofibers have provided the first and only evidence of a strategy to reverse RPP. Ultimately, we will evaluate composite nanofibers consisting of PCL and chitosan or PCL and collagen etc., since these combinations seem to afford an even more conducive environment for growth. In our studies here, PCL nanofibers provided a solid foundation or anchoring system upon which genetically modified cells resume normal functions and rescue the RPP. In addition, the fiber-recovered cells can be extracted, replated, and show signs of normal eGFP expression and growth.

A well-established cell-based system has been used to demonstrate that the general restriction of growth, observed in

genetically modified cells, can be reversed using biodegradable nanofibers. Electrospun PCL scaffolds support the recovery of these modified cells and enable DNA replication and cell division to take place. To our knowledge, this work is the first in which a biomaterial has been employed to overcome a critical barrier to the implementation of gene editing for the treatment of inherited diseases. We believe that these nanomaterials provide a supportive environment in which modified cells are enabled to proliferate. The proliferation of cells that bear a corrected genetic mutation is critical for many of the *ex-vivo* approaches envisioned in molecular medicine. Our combinatorial approach using biomaterials may accelerate this development.

## Materials and methods

**PCL nanofiber scaffolds fabrication.** Electrospun PCL nanofiber scaffolds were fabricated following the protocol described in Xie *et al.*<sup>16</sup> Briefly, PCL tablets (molecular weight = 80 kDa; Sigma-Aldrich, St Louis, MO) were dissolved in a solvent mixture consisting of dichloromethane and N,N-dimethylformamide (Fisher Chemicals, Waltham, MA) with a ratio of 4:1 (vol/vol) (at a concentration 10% (wt/vol)). Solutions were pumped at flow rate of 0.5 ml/hour using a syringe pump while a potential of 12 kV was applied between the spinneret (a 22-gauge needle) and a grounded collector located 12 cm away from the spinneret. A stainless steel frame containing an air gap (2 × 10 cm) was used to obtain parallel aligned nanofiber membranes. The nanofiber membrane, about 3.14 cm<sup>2</sup>, was glued to a microscope cover glass slip with medical grade silicone adhesive (NuSil Silicone Technology, Carpinteria, CA) followed by 8 minutes treatment in a plasma cleaner (PDC-32G; Harrick Plasma, Ithaca, NY) at a medium setting for surface hydrophilic modification. Then, the nanofiber scaffold was transferred into 6-well dishes, sterilized with 70% ethanol for several hours, rinsed with phosphate-buffered saline, and coated with 0.1% polylysine aqueous solution for 4–6 hours before cell seeding.

**Gene editing in HCT116-19 cells.** The integrated single-nucleotide mutation bearing eGFP gene of HCT116-19 cell line was corrected by means of the standard ssODN protocols.<sup>23,41</sup> Briefly, 2.5 × 10<sup>6</sup> cells were grown in 100 mm dishes in Hyclone McCoy's 5A complete medium (Thermo Scientific, Logan, UT) containing 6 μmol/l aphidicholin for synchronization. After 24 hours of synchronization, the cells were released from aphidicholin for 4 hours, harvested, rinsed with phosphate-buffered saline, and resuspended in Hyclone McCoy's 5A serum free medium. One million cells in 100 μl were then mixed with 3'-phosphorothioate-modified 72 NT ssODN (4 μmol/l final concentration) in a 4 mm gap electroporation cuvette (Fisher Scientific, Pittsburgh, PA) for electroporation. The sequence of the 72 NT ssODN (Integrated DNA Technologies, Coralville, IA) and the segment of its targeting non-functional eGFP gene sequence are shown in Figure 1. The cells were electroporated using a BTX Electro Square Porator ECM 830 (BTX Instrument Division, Holliston, MA) with settings of 250 V, 13 ms, 2 pulses, 1-second interval, followed by transfer onto nanofiber membrane covered microscope cover slip in a 6-well dish with 2 ml Hyclone McCoy's 5A complete medium for recovery and growth.

**FACS analysis of gene correction efficiency.** Seven sets (triplicates in each, totaling 21) of gene-editing reactions were carried out simultaneously and the cells were plated in 6-well dishes to examine correction efficiency and proliferation between 24 and 168 hours (8-day span). Twenty-four hours after the gene correction experiments were conducted, triplicates of samples were picked, and cells were harvested by trypsinization, pelleted, and resuspended in FACS buffer (Millipore, Temecula, CA) for FACS analysis. Every 24 hours following the first FACS analysis, another set of triplicates were picked and were analyzed for the gene-editing activity for the corresponding timepoint. The proportion of green fluorescence cells over total cells, the correction efficiency was analyzed using Guava EasyCyte 5HT Flow Cytometer software (Millipore). The seven data sets were plotted to demonstrate the gene-editing efficiency, cell survival, and proliferation over time.

**Fluorescence microscopy.** As described in the previous sections,  $1 \times 10^6$  HCT116-19 cells were electroporated with 72 NT ssODN followed by being seeded onto polylysine-coated electrospun aligned PCL nanofiber scaffolds in 6-well dishes or on the polylysine-coated dish surfaces. Beginning from the 24-hour post-electroporation timepoint, the cells were examined using a Zeiss Axiovert 25 CFL inverted light microscope (Zeiss) for proliferation and expansion on the polylysine-coated nanofiber scaffolds and dish surfaces; both transmitted and fluorescent reflected light features were employed. Once areas of cell proliferation were identified on the nanofiber scaffolds, the same sites were observed continually to monitor their expansion. Both the fluorescence and transmitted images were taken at the corresponding timepoints and the two images were overlapped for better visualization. For examination of cell attachment to the nanofibers, Leica SP5 TCSII multiphoton confocal microscope (Leica Microsystems, Buffalo Grove, IL) was used and side-view images were generated.

**HCT116-19 cell proliferation and Click-iT EdU assay.** Since the Click-iT EdU assay is one of the most sensitive and valid ways to detect active replication as a function of EdU incorporation into newly synthesized DNA, it is an excellent indirect way of assessing cell proliferation. We carried out gene-editing reactions on HCT116-19 cells as described above, plated the cells onto both polylysine-coated electrospun PCL nanofiber scaffolds and polylysine-coated 6-well dishes. Seventy-two hours after plating the cells, when the green cells started proliferation on the nanofibers, Click-iT assay was conducted on the adherent cells to determine the DNA replication activity in the dividing cells. Experimental procedures were conducted according to the manufacturer's instruction with an extra step of anti-eGFP labeling. Briefly, cells were labeled with EdU for 60 minutes, washed with  $1 \times$  wash buffer, and fixed for 20 minutes at room temperature. After fixation, cells were washed with wash buffer, and permeabilized for 20 minutes at room temperature. Anti-eGFP Alexa Fluor 488 antibody was used to label the eGFP protein expressed in the gene-edited HCT116-19 cells since the natural fluorescence of eGFP would be quenched by  $\text{Cu}^{2+}$  of the Click-iT assay reagent. The cells were fixed again with 3.7% paraformaldehyde/phosphate-buffered saline for 15 minutes to secure the anti-eGFP labeling followed by washing. Then, anti-EdU Alexa Fluor 647 antibody was added into the adherent cells and incubated at

room temperature for 1 hour. After the incubation, the cells were washed with assay buffer and examined under EVOS FL microscope (AMG Micro, Bothell, WA) to assess the EdU incorporation in replicating DNA.

**Acknowledgments.** We thank Cheresse Winstead (Delaware State University) for advice on the polymer reactions. We thank Hacene Boukari (Delaware State University) for assistance with the imaging of nanofibers. This work was supported partially by National Institutes of Health grant 5R01CA089325-12. The authors declared no conflict of interest.

1. Kubinová, S and Syková, E (2010). Nanotechnologies in regenerative medicine. *Minim Invasive Ther Allied Technol* **19**: 144–156.
2. Perán, M, García, MA, López-Ruiz, E, Bustamante, M, Jiménez, G, Madeddu, R et al. (2012). Functionalized nanostructures with application in regenerative medicine. *Int J Mol Sci* **13**: 3847–3886.
3. Vasita, R and Katti, DS (2006). Nanofibers and their applications in tissue engineering. *Int J Nanomedicine* **1**: 15–30.
4. Li, WJ, Laurencin, CT, Caterson, EJ, Tuan, RS and Ko, FK (2002). Electrospun nanofibrous structure: a novel scaffold for tissue engineering. *J Biomed Mater Res* **60**: 613–621.
5. Geng, X, Kwon, OH and Jang, J (2005). Electrospinning of chitosan dissolved in concentrated acetic acid solution. *Biomaterials* **26**: 5427–5432.
6. Li, C, Vepari, C, Jin, HJ, Kim, HJ and Kaplan, DL (2006). Electrospun silk-BMP-2 scaffolds for bone tissue engineering. *Biomaterials* **27**: 3115–3124.
7. Li, M, Mondrinos, MJ, Gandhi, MR, Ko, FK, Weiss, AS and Lelkes, PI (2005). Electrospun protein fibers as matrices for tissue engineering. *Biomaterials* **26**: 5999–6008.
8. Yoshimoto, H, Shin, YM, Terai, H and Vacanti, JP (2003). A biodegradable nanofiber scaffold by electrospinning and its potential for bone tissue engineering. *Biomaterials* **24**: 2077–2082.
9. Tuan, RS, Boland, G and Tuli, R (2003). Adult mesenchymal stem cells and cell-based tissue engineering. *Arthritis Res Ther* **5**: 32–45.
10. Li, WJ, Tuli, R, Okafor, C, Derfoul, A, Danielson, KG, Hall, DJ et al. (2005). A three-dimensional nanofibrous scaffold for cartilage tissue engineering using human mesenchymal stem cells. *Biomaterials* **26**: 599–609.
11. Jin, HJ, Chen, J, Karageorgiou, V, Altman, GH and Kaplan, DL (2004). Human bone marrow stromal cell responses on electrospun silk fibroin mats. *Biomaterials* **25**: 1039–1047.
12. Riboldi, SA, Sampaolesi, M, Neuenschwander, P, Cossu, G and Mantero, S (2005). Electrospun degradable polyesterurethane membranes: potential scaffolds for skeletal muscle tissue engineering. *Biomaterials* **26**: 4606–4615.
13. Xie, J, Willerth, SM, Li, X, Macewan, MR, Rader, A, Sakiyama-Elbert, SE et al. (2009). The differentiation of embryonic stem cells seeded on electrospun nanofibers into neural lineages. *Biomaterials* **30**: 354–362.
14. Yang, F, Xu, CY, Kotaki, M, Wang, S and Ramakrishna, S (2004). Characterization of neural stem cells on electrospun poly(L-lactic acid) nanofibrous scaffold. *J Biomater Sci Polym Ed* **15**: 1483–1497.
15. Yang, F, Murugan, R, Wang, S and Ramakrishna, S (2005). Electrospinning of nano/micro scale poly(L-lactic acid) aligned fibers and their potential in neural tissue engineering. *Biomaterials* **26**: 2603–2610.
16. Xie, J, MacEwan, MR, Li, X, Sakiyama-Elbert, SE and Xia, Y (2009). Neurite outgrowth on nanofiber scaffolds with different orders, structures, and surface properties. *ACS Nano* **3**: 1151–1159.
17. Bhardwaj, N and Kundu, SC (2010). Electrospinning: a fascinating fiber fabrication technique. *Biotechnol Adv* **28**: 325–347.
18. Reneker, DH, Kataphinan, W, Theron, A, Zussman, E and Yarin, AL (2002). Nanofiber garlands of polycaprolactone by electrospinning. *Polymer* **43**: 6785–6794.
19. Venugopal, J, Zhang, YZ and Ramakrishna, S (2005). Fabrication of modified and functionalized polycaprolactone nanofiber scaffolds for vascular tissue engineering. *Nanotechnology* **16**: 2138–2142.
20. Schnell, E, Klinkhammer, K, Balzer, S, Brook, G, Klee, D, Dalton, P et al. (2007). Guidance of glial cell migration and axonal growth on electrospun nanofibers of poly-epsilon-caprolactone and a collagen/poly-epsilon-caprolactone blend. *Biomaterials* **28**: 3012–3025.
21. Ghasemi-Mobarakeh, L, Prabhakaran, MP, Morshed, M, Nasr-Esfahani, MH and Ramakrishna, S (2008). Electrospun poly(epsilon-caprolactone)/gelatin nanofibrous scaffolds for nerve tissue engineering. *Biomaterials* **29**: 4532–4539.
22. Engstrom, JU, Suzuki, T and Kmiec, EB (2009). Regulation of targeted gene repair by intrinsic cellular processes. *Bioessays* **31**: 159–168.
23. Hu, Y, Parekh-Olmedo, H, Drury, M, Skogen, M and Kmiec, EB (2005). Reaction parameters of targeted gene repair in mammalian cells. *Mol Biotechnol* **29**: 197–210.
24. Papaioannou, I, Disterer, P and Owen, JS (2009). Use of internally nuclease-protected single-strand DNA oligonucleotides and silencing of the mismatch repair protein, MSH2, enhances the replication of corrected cells following gene editing. *J Gene Med* **11**: 267–274.
25. Olsen, PA, Randol, M and Krauss, S (2005). Implications of cell cycle progression on functional sequence correction by short single-stranded DNA oligonucleotides. *Gene Ther* **12**: 546–551.

26. Olsen, PA, Randol, M, Luna, L, Brown, T and Krauss, S (2005). Genomic sequence correction by single-stranded DNA oligonucleotides: role of DNA synthesis and chemical modifications of the oligonucleotide ends. *J Gene Med* **7**: 1534–1544.
27. Huen, MS, Li, XT, Lu, LY, Watt, RM, Liu, DP and Huang, JD (2006). The involvement of replication in single stranded oligonucleotide-mediated gene repair. *Nucleic Acids Res* **34**: 6183–6194.
28. Aarts, M and te Riele, H (2010). Parameters of oligonucleotide-mediated gene modification in mouse ES cells. *J Cell Mol Med* **14**(6B): 1657–1667.
29. Radecke, S, Radecke, F, Peter, I and Schwarz, K (2006). Physical incorporation of a single-stranded oligodeoxynucleotide during targeted repair of a human chromosomal locus. *J Gene Med* **8**: 217–228.
30. Bertoni, C, Morris, GE and Rando, TA (2005). Strand bias in oligonucleotide-mediated dystrophin gene editing. *Hum Mol Genet* **14**: 221–233.
31. Urov, FD, Rebar, EJ, Holmes, MC, Zhang, HS and Gregory, PD (2010). Genome editing with engineered zinc finger nucleases. *Nat Rev Genet* **11**: 636–646.
32. Carroll, D (2008). Progress and prospects: zinc-finger nucleases as gene therapy agents. *Gene Ther* **15**: 1463–1468.
33. Cermak, T, Doyle, EL, Christian, M, Wang, L, Zhang, Y, Schmidt, C et al. (2011). Efficient design and assembly of custom TALEN and other TAL effector-based constructs for DNA targeting. *Nucleic Acids Res* **39**: e82.
34. Miller, JC, Tan, S, Qiao, G, Barlow, KA, Wang, J, Xia, DF et al. (2011). A TALE nuclease architecture for efficient genome editing. *Nat Biotechnol* **29**: 143–148.
35. Wood, AJ, Lo, TW, Zeitler, B, Pickle, CS, Ralston, EJ, Lee, AH et al. (2011). Targeted genome editing across species using ZFNs and TALENs. *Science* **333**: 307.
36. Aarts, M and te Riele, H (2011). Progress and prospects: oligonucleotide-directed gene modification in mouse embryonic stem cells: a route to therapeutic application. *Gene Ther* **18**: 213–219.
37. Parekh-Olmedo, H and Kmiec, EB (2007). Progress and prospects: targeted gene alteration (TGA). *Gene Ther* **14**: 1675–1680.
38. Ferrara, L and Kmiec, EB (2006). Targeted gene repair activates Chk1 and Chk2 and stalls replication in corrected cells. *DNA Repair (Amst)* **5**: 422–431.
39. Engstrom, JU and Kmiec, EB (2007). Manipulation of cell cycle progression can counteract the apparent loss of correction frequency following oligonucleotide-directed gene repair. *BMC Mol Biol* **8**: 9.
40. Ferrara, L, Engstrom, JU, Schwartz, T, Parekh-Olmedo, H and Kmiec, EB (2007). Recovery of cell cycle delay following targeted gene repair by oligonucleotides. *DNA Repair (Amst)* **6**: 1529–1535.
41. Bonner, M and Kmiec, EB (2009). DNA breakage associated with targeted gene alteration directed by DNA oligonucleotides. *Mutat Res* **669**: 85–94.
42. Liu, C, Wang, Z, Huen, MS, Lu, LY, Liu, DP and Huang, JD (2009). Cell death caused by single-stranded oligodeoxynucleotide-mediated targeted genomic sequence modification. *Oligonucleotides* **19**: 281–286.
43. Bonner, M, Strouse, B, Applegate, M, Livingston, P and Kmiec, EB (2012). DNA damage response pathway and replication fork stress during oligonucleotide directed gene editing. *Mol Ther* **1**: e18.
44. Gerardo-Nava, J, Führmann, T, Klinkhammer, K, Seiler, N, Mey, J, Klee, D et al. (2009). Human neural cell interactions with orientated electrospun nanofibers in vitro. *Nanomedicine (Lond)* **4**: 11–30.
45. Zhang, YZ, Venugopal, J, Huang, ZM, Lim, CT and Ramakrishna, S (2005). Characterization of the surface biocompatibility of the electrospun PCL-collagen nanofibers using fibroblasts. *Biomacromolecules* **6**: 2583–2589.
46. Gamper, HB Jr, Cole-Strauss, A, Metz, R, Parekh, H, Kumar, R and Kmiec, EB (2000). A plausible mechanism for gene correction by chimeric oligonucleotides. *Biochemistry* **39**: 5808–5816.
47. Drury, MD and Kmiec, EB (2003). DNA pairing is an important step in the process of targeted nucleotide exchange. *Nucleic Acids Res* **31**: 899–910.
48. Tillman, BW, Yazdani, SK, Lee, SJ, Geary, RL, Atala, A and Yoo, JJ (2009). The in vivo stability of electrospun polycaprolactone-collagen scaffolds in vascular reconstruction. *Bio-materials* **30**: 583–588.



**Molecular Therapy–Nucleic Acids** is an open-access journal published by Nature Publishing Group. This work is licensed under the Creative Commons Attribution-NonCommercial-No Derivative Works 3.0 Unported License. To view a copy of this license, visit <http://creativecommons.org/licenses/by-nc-nd/3.0/>